Lithosphere destabilization and small-scale convection constrained from geophysical data and analogical models

Supplementary material

C. Adam[1], V. Vidal[2], B. Pandit[1], A. Davaille[3], and P.D. Kempton[1]

[1] Geology Department, Kansas State University of Agriculture and Applied Science, Kansas, USA
[2] Laboratoire de Physique, CNRS UMR 5672, Ecole Normale Supérieure de Lyon, Lyon, France
[3] FAST laboratory, Orsay University, Orsay, France

The supplementary online material contains additional information on the method developed to determine the base of the lithosphere from tomography models. The influence of the parameters chosen for this determination is also discussed.

1. Influence of the parameters on the determination of the base of the lithosphere from an isovalue of the seismic velocity anomalies

1.1 Method

In this section, we explain in more details the method developed to extract the base of the oceanic lithosphere from an isovalue of the seismic velocity anomalies, and discuss the influence of the parameters on the final results. The base of the lithosphere will be referred hereafter as LAB (Lithosphere Asthenosphere Boundary). As stated in the main paper, we determine the base of the lithosphere from the SEMUCB-WM1 seismic tomography models (French and Romanowicz, 2014). Seismic tomography models provide a snapshot of the internal structure of the Earth, in terms of seismic velocity variations, *dvs*. In ocean basins, *dvs* values are relatively higher in the shallowest 100-150 km (blue areas in Figure S1a,b), translating the fact that the lithosphere is colder and compositionally distinct when compared to the underlying mantle. To determine the base of the lithosphere, we consider for each point, i.e. for each longitude/latitude at the surface of the globe, *dvs* versus depth profiles, similar to the profile displayed in Figure S1c. We consider only depths between 50 and 180 km, (shaded area in Figure S1c) for reasons discussed in section 1.2. Along this profile we select the depth for which the *dvs* is the closest to the *dvs* we select as

representative of the base of the lithosphere (*dvs*=1.5% in this case). This point is represented by a blue star in Figure S1c. The *dvs* we select as representative of the base of the lithosphere is a parameter of the model, and will be discussed in section 1.4.

The *dvs*=1.5% isosurface we obtain is represented in Figure S1d and in the depth cross sections in Figure S1a,b (white lines). There are some regions in which the lithosphere cannot actually be "seen" from tomography models. In particular, near mid-oceanic ridges (MOR), the tomography shows broad regions characterized by slow seismic velocities (Figure S1a,b). These seismically slow regions correspond to partially melted mantle rising at spreading centers to form the new oceanic plates. In these case, the base of the lithosphere cannot be determined because the lithosphere is not visible in the tomography models. These regions are represented in gray in the final map (Figure S1e).

Along the older parts of the lithosphere, in the North West Pacific, the lithosphere appears as a seismically fast region (blue shallow region between longitudes 145 and 200°E along the AA' depth cross sections (Figure S1a). The lower boundary of the lithosphere is generally well recovered by the white line, but in some regions there are sharp variations in the depth of the LAB. This is due to the fact that dvs=1.5% value can be encountered in shallower regions than the base of the lithosphere. However, as these regions are outliers, they can be easily eliminated. To remove these small scale variations, we remove the points for which the spatial derivative of the lithosphere base $\delta_{depth}/\delta_{dist}$ is greater than a threshold value, *tv*. This threshold value is a parameter of the model, and will be discussed in section 1.3. In the following, we present results obtained with *tv=500*. We then interpolate the points for which the base of the lithosphere was successfully determined with the "griddata" function, available in Matlab (Matlab R2016b, Mathworks®). This function has interpolation parameters that will be discussed in section 1.4. Our final estimate of the depth of the base of the lithosphere is displayed in Figure S1e. This depth is reported by a red dashed line in the depth cross sections represented in Figure S1a,b. The anomalies evidenced along the oldest oceanic lithosphere are similar in Figures S1d. This is due to the fact that the second and final step of our method (Figure S1e) only eliminates regions where the lithosphere is not "seen" in the tomography model (such as near mid-oceanic ridges), and removes the sharp variations of the surface defining the base of the lithosphere.

For each latitude/longitude, we then obtain the depth of the lithosphere-asthenosphere boundary, when this boundary can actually be seen in the SEMUCB-WM1 tomography model (i.e. at the exception of the regions represented in gray on Figure S1e). Our study focuses on the Pacific plate, which is the largest tectonic plate, and is entirely oceanic.

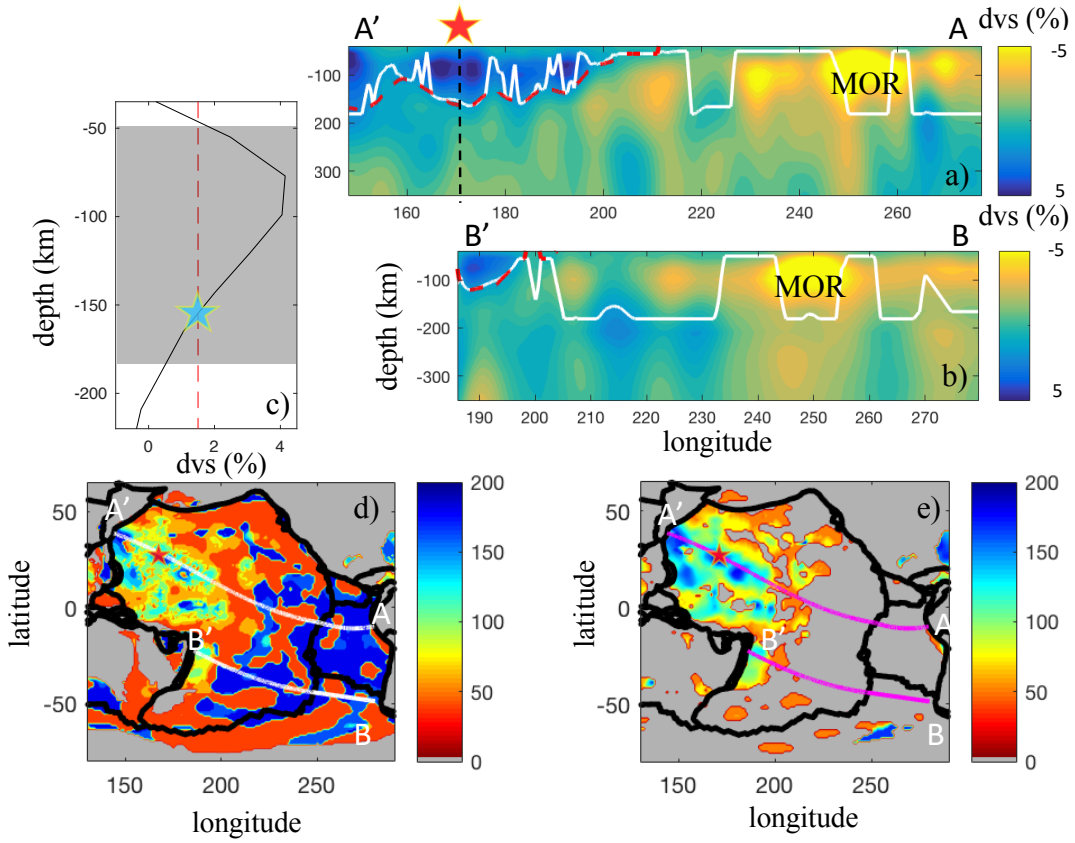

Figure S1: Method for obtaining the base of the lithosphere from an isovalue of the seismic velocity anomaly (dvs=1.5%). a) and b) depth cross sections across the SEMUCB-WM1 tomography model (French and Romanowicz, 2014) along the profiles reported in panel d) and e). The white and dashed red line illustrate the result of the first second step our method respectively. c) *dvs* versus depth profile at longitude 170°E and latitude 27°N. This location is represented by a red star in panels a, d and e. The shaded area represents the 50-180 km depth range considered in this study. The blue star represents the point for which the *dvs* is the closest to 1.5%. The color maps displayed in panels d and e represent the depth of the LAB obtained through the first and second step of our approach respectively. The AA' and BB' profiles represent the present-day plate motion direction. They have been computed by using the Nuvel1A model, in the HS3 reference frame (Gripp and Gordon, 2002). The black thick lines in panels d) and e) are plates boundaries, taken from Bird (2003)

In the following sections, we will discuss the effects of varying the parameters for the determination of the LAB. We will also compare several tomography models to our "reference" or "favorite" model (Figure S1e), obtained by considering the SEMUCB-WM1 tomography model (French and Romanowicz, 2014). We remind here the parameters used to obtain this model: dvs=1,5%, *tv=500*, a linear interpolation to obtain a continuous grid. When testing the influence of one parameter (the depth range for example), the other model parameters will be kept constant and identical to the reference model (detailed above). Unless specified, the profiles displayed in the Pacific maps in the SOM represent the present-day plate motion direction and have been computed by using the Nuvel1A model, in the HS3 reference frame (Gripp and Gordon, 2002; Adam et al., 2015).

1.2 Influence of the depth range

To determine the base of the lithosphere, we consider for each point, i.e. for each longitude/latitude at the surface of the globe, *dvs* versus depth profiles (Figure S1c). The shallowest depth described by the SEMUCB-WM1 tomography model is 35 km. The oceanic lithosphere is characterized by positive dvs (blue regions in Figures S2a,b. The maximum *dvs* are however located in the middle of the lithosphere, as seen shown in Figures S1a,b,c and S2a,b. In order to avoid extracting the upper limit of the lithosphere, we will only consider depths greater than 50 km. In Figure S2c we show the map of the base of the lithosphere computed by considering the 35-180 km depth range. We compare it to the reference model computed by considering the 50-180 km depth range (Figure S1e). The difference between these two estimates, displayed in Figure S2d, is generally null, at the exception of a few regions. The AA' profile intersects a maximum in the difference map. Along this profile we display the depth cross section across the SEMUCB-WM1 tomography model, and report the two estimates of the LAB (Figure S2a). The LAB computed by considering the 50-180 km depth range, reported in white, follows the base of the lithosphere, while the LAB computed by considering the 35-180 km depth range, reported by the red dashed line selects the upper limit of the lithosphere for longitudes 145-155^{o}E, i.e. around point A'. Considering shallower depths does not change the pattern of the LAB (Figure S1a, Figure S2a) and introduces only a few local differences (Figure S2b).Considering depths larger than 50 km is thus more adequate as it makes possible to select correctly the lower limit of the lithosphere. The maximal depth considered for

dvs versus depth profiles is 180 km. Varying this maximal depth between depths 180 and 200 km does not have significant effects on the determination of the LAB. However, if this maximal depth is 220 km or larger, the surface corresponding to dvs=1.5% selects anomalies located well beyond the lithosphere and even beneath the asthenosphere (Figure S2b, pink profile). In the following we will discuss LAB estimates computed by considering the 50-180 km depth range.

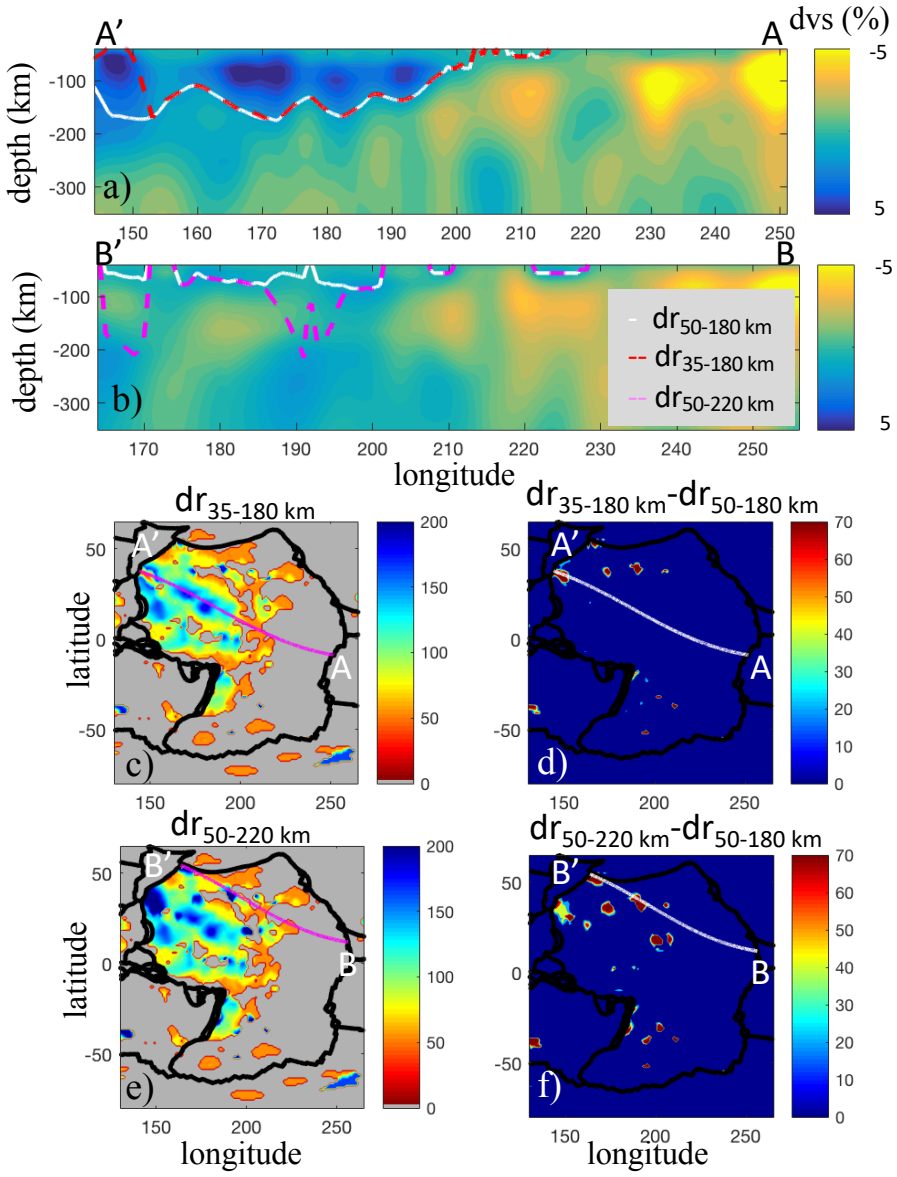

Figure S2: Influence of the considered depth range on the computation of the LAB depth. a) and b) depth cross sections across the SEMUCB-WM1 tomography model along the profiles reported in panels c-f. The color lines represent our models of the LAB (color code is in the figure). The color maps displayed in panels c and e represent the depth of the LAB obtained with the depth ranges 35-180 km, and 50-220 km respectively. The depth ranges, 'dr' are reported above each

panel. The absolute value of the difference between these models and the reference model (depth ranges 50-180 km) is displayed in panels d and f.

1.3 Influence of the threshold value for the LAB spatial derivative

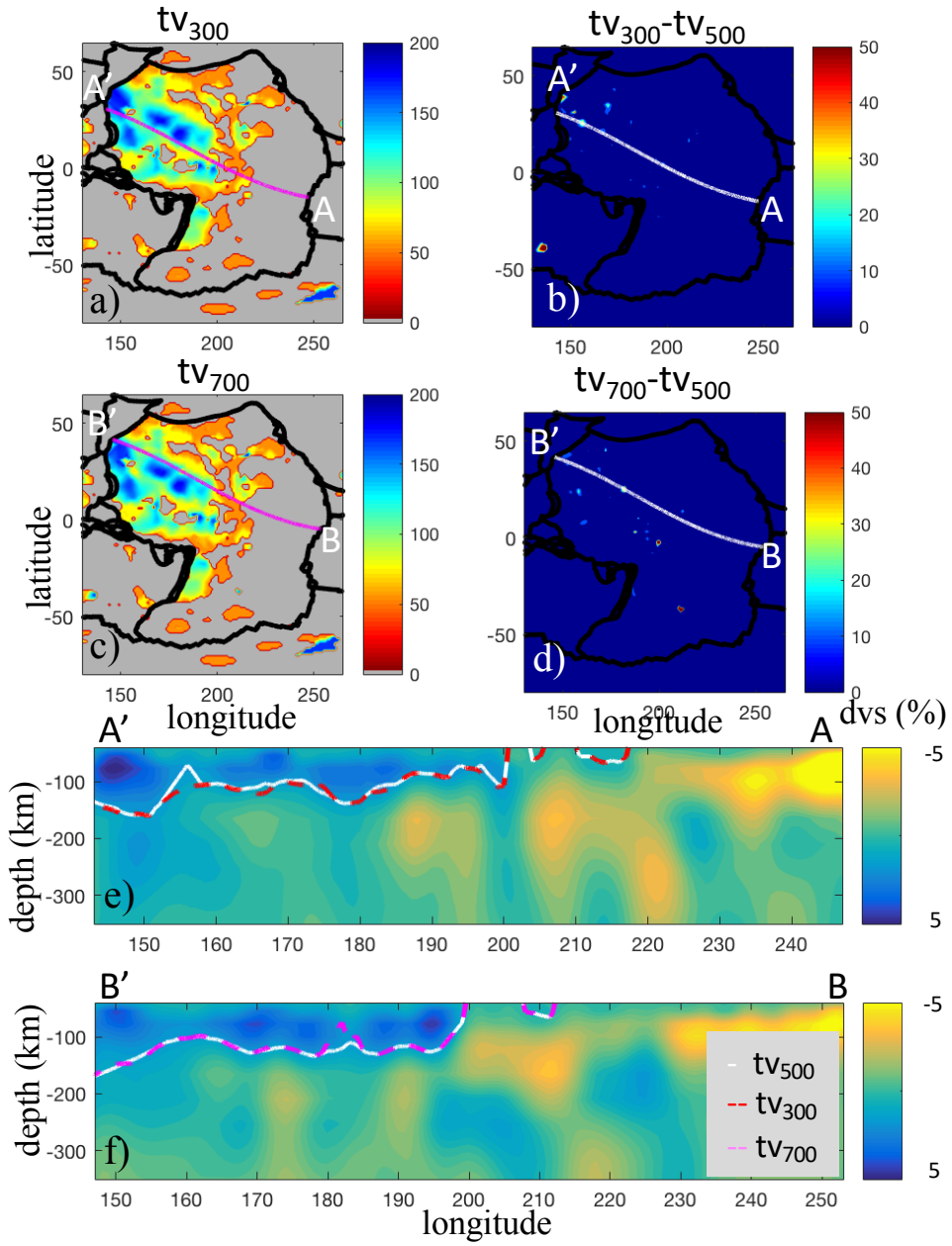

Figure S3: Influence of the threshold value, tv, for the LAB spatial derivative. The color maps displayed in panels a and c represent the depth of the LAB obtained with tv=300 and 700 respectively. The considered threshold value, tv, are reported above each panel. The absolute value of the difference between these models and the reference model (tv=500) is displayed in panels b and d. Depth cross sections of the tomography model (SEMUCB-WM1) along the AA' and BB'

profiles are reported in panels e and f. The color lines represent our models of the LAB (color code is in the figure).

The surface obtained by selecting the depths for which the *dvs* is closest to 1.5% displays some sharp variations locally, due to the fact that dvs=1.5% value can be encountered in shallower regions than the base of the lithosphere (Figure S1e). To remove these small scale variations, corresponding to outliers, we remove the points for which the spatial derivative of the lithosphere base $\delta_{depth}/\delta_{dist}$ is greater than a threshold value, *tv*. To derive the LAB map displayed in Figure S1e, we have used a threshold value of 500. This means that we only consider the points for which a 100 km variation in the LAB depth occurs over a lateral distance of 500 km or more. Varying this threshold value between 300 and 700 does not have a major influence on the estimation of the LAB, as shown in Figure S3 (*tv* is indicated above each panel). The LAB computed with tv=300 and 700 (Figure S3 a and c respectively does not display any significant differences from the LAB computed with tv=500 (Figure S1a).

1.4 Influence of the interpolation parameters

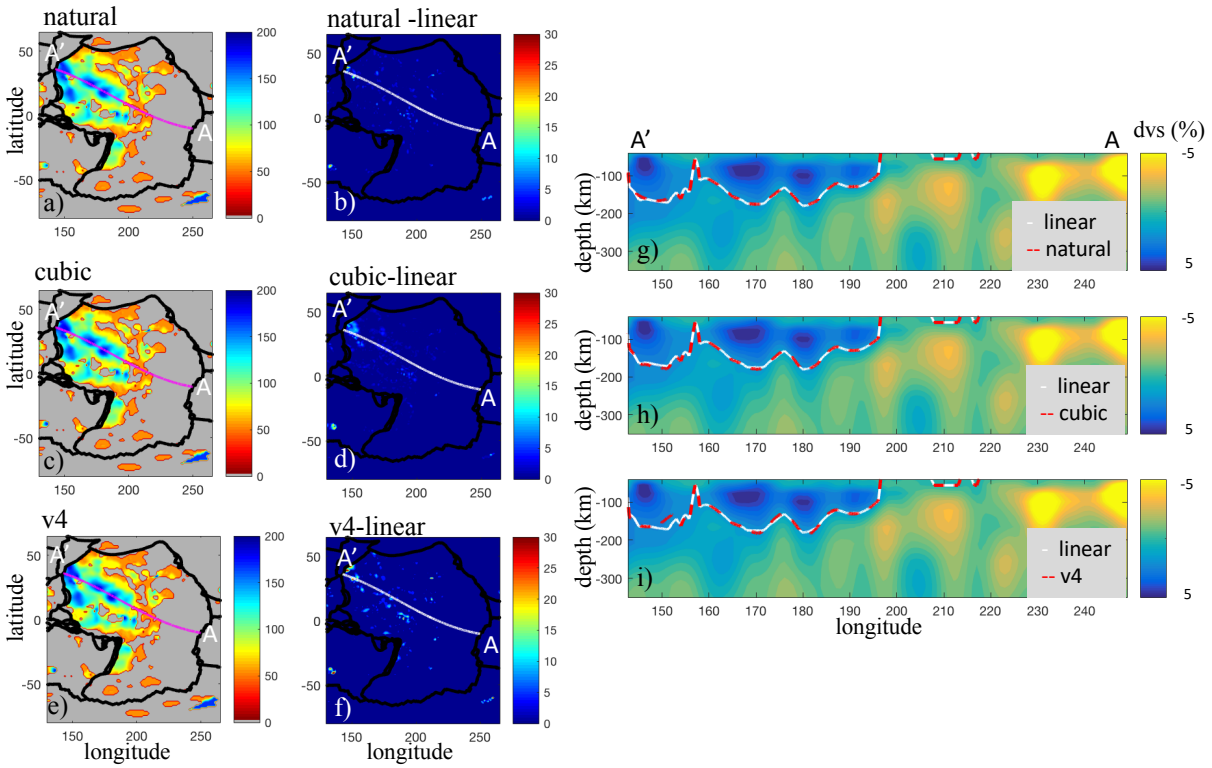

Figure S4: Influence of the interpolation parameters. The color maps displayed in panels a, c and e represent the depth of the LAB obtained with different interpolation methods reported above

each panel. The absolute values of the difference between these models and the reference model are displayed in panels b, d and f. Depth cross sections across the tomography model (SEMUCB-WM1) along the AA' profile are reported in panels g, h and i.

After selecting the depths for which the dvs is closest to dvs=1.5% and removing the outliers (section 1.3), we interpolate the remaining points with the "griddata" function from Matlab (Matlab R2016b, Mathworks®), in order to obtain a continuous grid. In Figure S4 we study the influence of the interpolation method. The LABs displayed in Figure S4, in panels a, c, and e, have been obtained with different interpolation methods reported above each panel, are very similar to the reference LAB, (Figure S1e), computed with the linear interpolation. There are indeed only local departures, with amplitudes smaller than 20 km (Figure S4b,d,f).

1.5 Influence of dvs representing the base of the lithosphere.

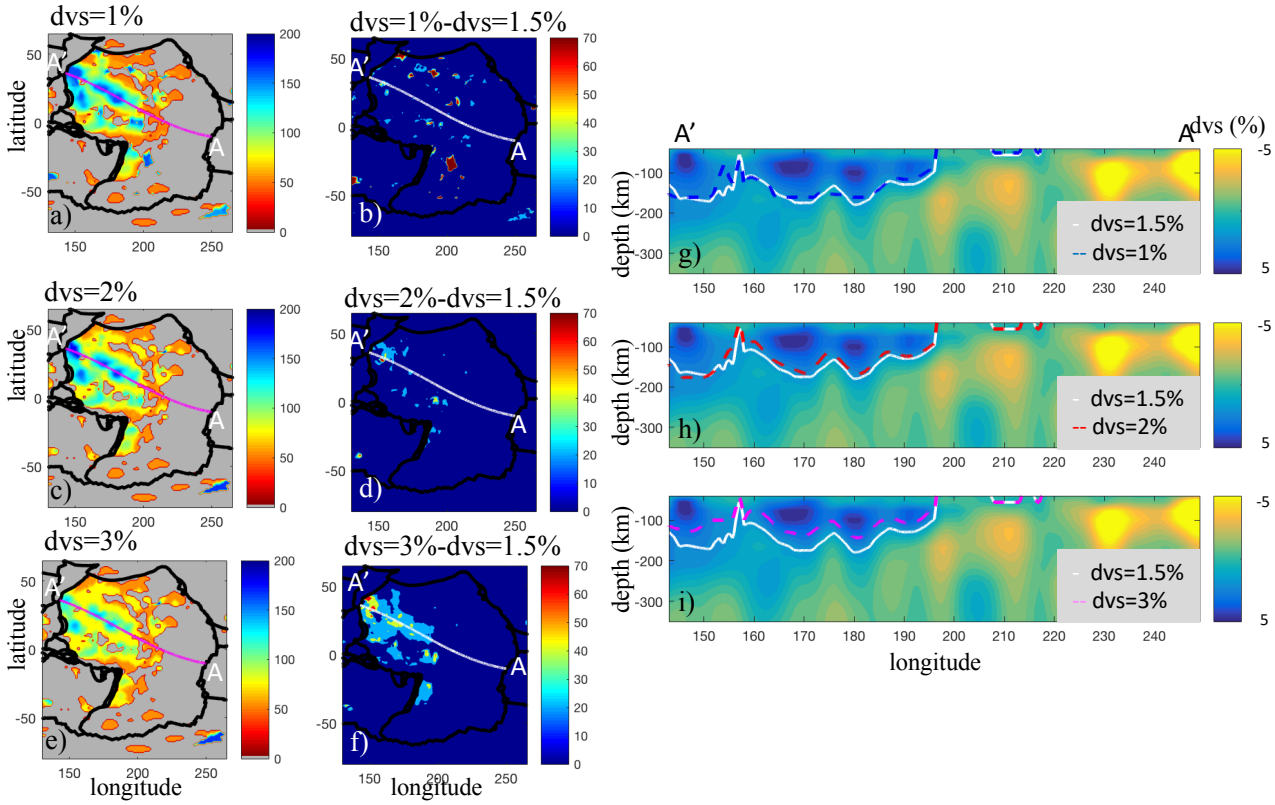

Figure S5: Influence of the dvs representative of the base of the lithosphere. The color maps displayed in panels a, c and e represent the depth of the LAB obtained with different dvs, reported above each panel. The absolute values of the difference between these models and the reference model (dvs=1.5%) are displayed in panels b, d and f. Depth cross sections across the tomography

model (SEMUCB-WM1) along the AA' profile are reported in panels g, h and i. The color lines represent our models of the LAB (color code is in the figure).

As stated in the main paper, there is no consensus on the *dvs* representative of the base of the lithosphere. In Figures S1-S4, the base of the lithosphere seems to be between *dvs*=1 % and *dvs*=2 %. As these numbers cannot be constrained, we test in Figure S5 the influence of the choice of the *dvs* representative of the base of the lithosphere. We test *dvs* values of 1, 2 and 3 %. We compare the base of the lithosphere computed with these values to the base of the lithosphere obtained with *dvs*=1.5 % (Figure S1e). Within this range, the choice of the *dvs* representative of the base of the lithosphere does not have a major influence on the shape of the base of the lithosphere. The chosen *dvs* value will slightly influence the depth of the base of the lithosphere, but not the location of patterns at its base, which is the topic of this study.

2. Determination of the base of the lithosphere from an isotherm

The definition of the lithosphere depends on its physical and chemical properties. For example, the mechanical thickness is defined in seismology as the layer where the seismic waves propagate without attenuation (Isacks et al., 1968). The elastic thickness, which characterizes the behavior of the lithosphere on geological time scales is 50% smaller than the mechanical thickness (McNutt, 1984; Nishimura et Forsyth, 1985). Other studies define the lithosphere as a function of its rheology (Goetze, 1979; Bodine et al., 1981; McNutt et Menard, 1982). When the lithosphere is defined as the boundary layer of mantle convection, one talks about thermal thickness of the lithosphere.

The isotherm defining the base of the lithosphere depends then on the considered physical properties. The base of the mechanical lithosphere is defined by the 1400 K isotherm according to Schubert et al. (2001). The base of the thermal lithosphere corresponds to the 1350±275°C (1623±275K) isotherm according to (Parsons et Sclater, 1977). For Stein and Stein (1992), it corresponds to the 1350±275°C (1623±275K) isotherm. The base of the lithosphere could then be defined by an isotherm. This would avoid the subjectivity related to an ad-hoc choice of the *dvs* representing the base of the lithosphere. However, the isotherm defining the base of the lithosphere

is still debated (see discussion above). Moreover, the calculation of this isotherm from tomography models requires other parameters, which are not all well constrained, as discussed below.

To convert the seismic velocity anomalies provided by tomography models, *dvs*, into temperature anomalies, *dT*, we use here the conversion factor, A_{VT} obtained by Karato (2008) from laboratory experiments (Figure S6a). The temperature anomaly, *dT*, is obtained by:

$$dT = \frac{dvs}{A_{VT}} \quad \text{(s1)}$$

To compute the temperature, *T*, we should then add a 1D temperature profile, T_{ref}, to the *dT* field.

$$T = dT + T_{ref} \quad \text{(s2)}$$

There are numerous models describing the thermal structure of the lithosphere. Two of the most widely-used models are the GDH1 (Global Depth and Heat Flow, Stein and Stein, 1992) and PS (Parsons et Sclater,1977) plate models. According to the PS model, the maximal lithosphere thickness is 125±10 km, and the bottom boundary temperature is 1350±275°C. For Stein and Stein (1992), the base of the lithosphere is better defined by the 1,450±250°C isotherm, and the asymptotic lithosphere thickness is 95 ± 15 km. The difference between these two models are the data sets considered to fit the plate model. These two 1D temperature profiles are reported in Figure S6b. The thermal gradient beneath the oceanic lithosphere varies between 0.3 and 0.5°/km according to Turcotte and Schubert (1982). Therefore, for depths greater than 95 and 125 km, we impose these thermal gradients (Figure 6b).

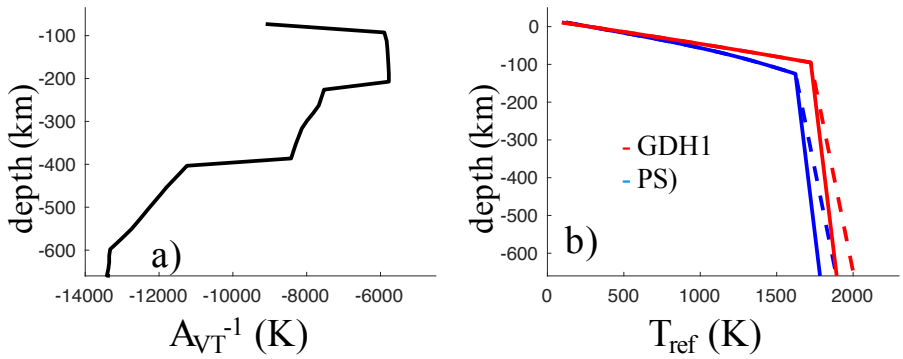

Figure S6: Parameters use to convert the seismic velocity anomalies provided by tomography models, dvs, in temperatures. a) $1/A_{VT}$ conversion factor obtained by Karato (2008); b) 1D

reference temperature profiles. GDH1 (Stein and Stein, 1992) and PS (Parsons et Sclater, 1977) are reported in red and blue respectively. Beneath the lithosphere, we impose a 0.3°/km thermal gradient (dashed blue and red lines) and 0.5°/km (full blue and red lines).

Using a 1D temperature profile is an over-simplification, based on the incorrect assumption that the thickness of the lithosphere is the same all along the oceanic plate. In theory, the lithosphere thickness is almost null near the oceanic ridges, and reaches ~100 km for old ages (Parsons et Sclater, 1977; Stein and Stein, 1992; Turcotte and Schubert, 1982). The definition of "old ages" differs according to the different authors. For Stein and Stein (1992), the lithosphere reaches its asymptotic thickness (95 ± 15 km) at 20 Myr. According to Parsons et Sclater (1977), the asymptotic thickness (125 ± 10 km) is reached at 50-70 Myr. Considering that the lithosphere is not actually "seen" in tomography models near mid-oceanic ridges (see discussion in section 1.1), using a 1D temperature profile becomes a valid assumption. However, the regions near mid-oceanic ridges should not be considered, as the lithosphere will be artificially introduced through the addition of the 1D temperature profile with a 100 km lithosphere. These regions will be masked in the following, as in Figure S1e.

In Figure S7 we test the influence of the considered 1D reference temperature profile on the computation of the depth of the lithosphere. The depth cross sections reported in Figure S7 represent the temperature field. They have been computed from the SEMUCB-WM1 tomography model. We use equation s1 to convert the seismic velocity into temperature anomaly. To convert the temperature anomaly in temperature, we use the 1D temperature profiles displayed in Figure S6b. As the definition of the isotherm defining the base of the lithosphere is still debated, we have reported two isotherms, 1500K and 1600K for each model. Varying the 1D temperature profile introduces noticeable variations on the recovered temperature fields (Figure S7a-c). The 1D reference temperature predicted by GDH1 (Stein and Stein, 1992) induces the hottest mantle for depths 100-350 km. As the temperature fields differ, so does the depth of the 1500K and 1600K isotherms. This can be observed in panels a-c, but can be better seen in panel e, where we reported the emplacement of all the 1500K isotherms. The difference between the models is in the order of 50-100 km. This is a huge difference considering that most of the models describe the lithosphere as a 100 km thick layer (Parsons et Sclater,1977; Stein and Stein, 1992).

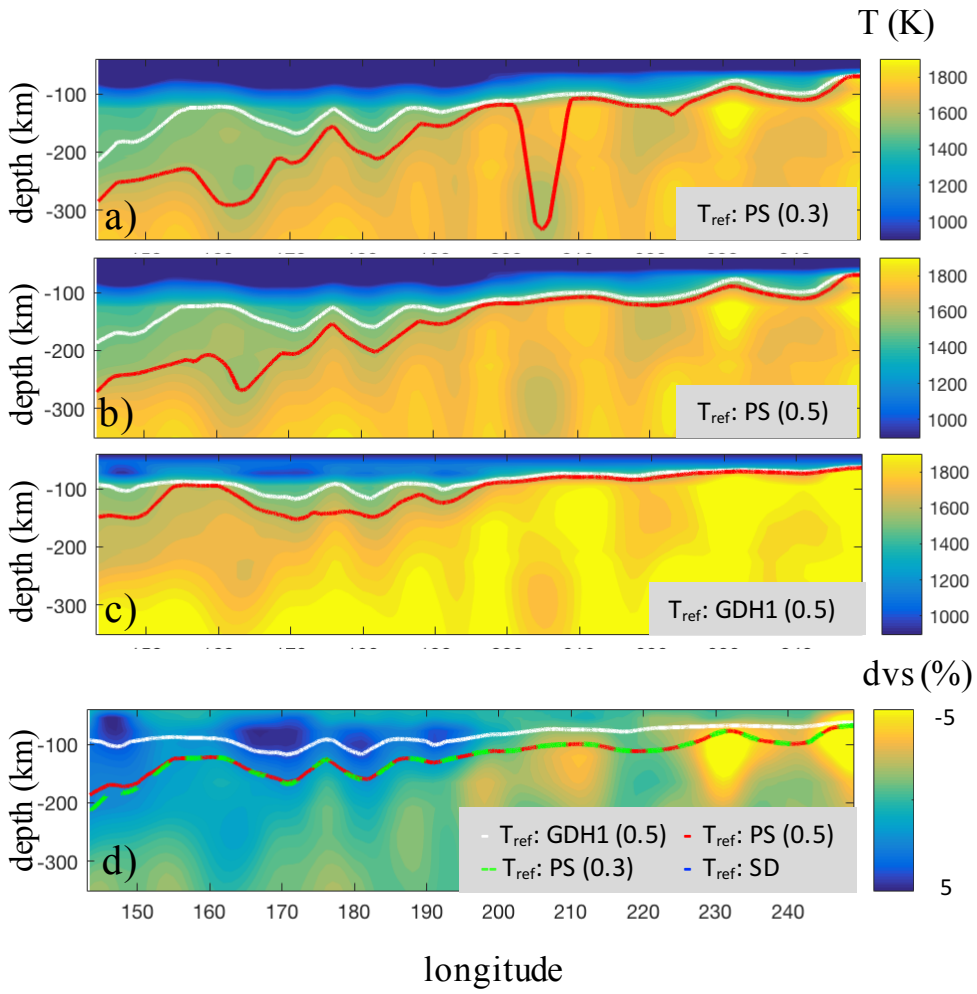

Figure S7: Influence of the 1D reference temperature profile for the conversion from *dvs* to temperature. Panels a-d are temperature fields interpolated along the AA' profile, which location is reported in Figure S1e. The temperature fields have been obtained from the 1D reference temperature profiles indicated in the panels. 0.3 and 0.5 describe the thermal gradient imposed beneath the lithosphere: a 0.3°/km or 0.5°/km. The white and red lines represent respectively the 1500K and 1600K isotherms, extracted for each model. In panel d the color lines represent the estimates of the 1500K obtained by varying the 1D reference temperature profiles (legend in the figure). The color map in panel d represents *dvs* variations.

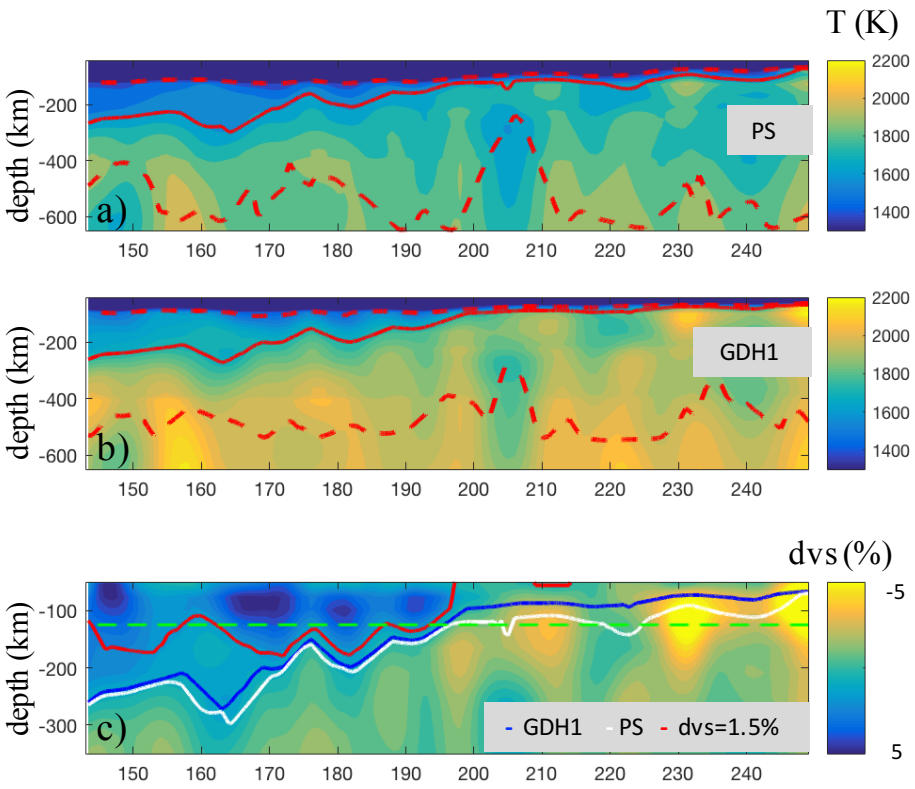

Figure S8: The color maps represent the temperature fields computed from models PS (a), and GDH1 (b), assuming a 0.5°/km thermal gradient beneath the lithosphere. The red lines represent the isotherms which better describe the lithosphere according to these models. The red dashed lines represent the uncertainties associated with these isotherms. The color map in panel c represents *dvs* variations, and the color lines estimates of the base of the lithosphere determined by various models (legend in the figure). The green dashed line corresponds to the 125 km depth.

The location of the isotherms presumably describing the base of the lithosphere according to the GDH1 and PS models are displayed in Figure S8 a and b. The isotherms are superimposed on the temperature fields computed with the 1D temperature profiles predicted by these models (Figure S6b). According to Stein and Stein (1992), the base of the lithosphere is better described by the 1450±250°C isotherm. For Parsons et Sclater (1977), the 1350±275°C isotherm is a better approximation. The upper and lower boundaries of these ranges are reported by the red dashed lines. The lower boundaries of both the PS and GDH1 models are unrealistic, as they reach depths of 500-600 km. The "central isotherms" are also improbable, as they predict the base of the lithosphere to be at depths larger than 200 km (Figure 8c), while this depth should in theory be in the 95-125 km range. The PS and GDH1 models predict indeed that the base of the lithosphere is

at depths 125+10 km and 95 ± 15 km respectively. The 125 km depth is reported in green in panel c. The base of the lithosphere determined by *dvs*=1.5% corresponds in average to 125 km at old ages, with variations corresponding to the lithospheric instabilities. The uncertainty associated with the depth is actually much smaller that the uncertainty associated with the isotherm in the PS and GDH1 models. According to these models, the range of possible isotherms defining the base of the lithosphere encompass values between 1348 and 1973 K.

In Figure S9, we investigate which isotherm corresponds to *dvs*=1.5%. While using the PS (05) 1D reference model, T_{ref}, the surface determined by *dvs*=1.5% corresponds roughly to the 1500 K isotherm. While using the GDH1 (05) 1D reference model, the surface defined by *dvs*=1.5% corresponds roughly to the 1650 K isotherm. As discussed earlier, converting the seismic velocity anomalies in temperature requires several parameters that are not very well constrained. This is the main reason for which we choose to present the base of the lithosphere derived from an isovalue of the seismic velocity anomaly. We also show that the isotherm corresponding to the *dvs=1.5%* isovalue (1500 K and 1650 K) correspond to realistic values proposed for the base of the lithosphere.

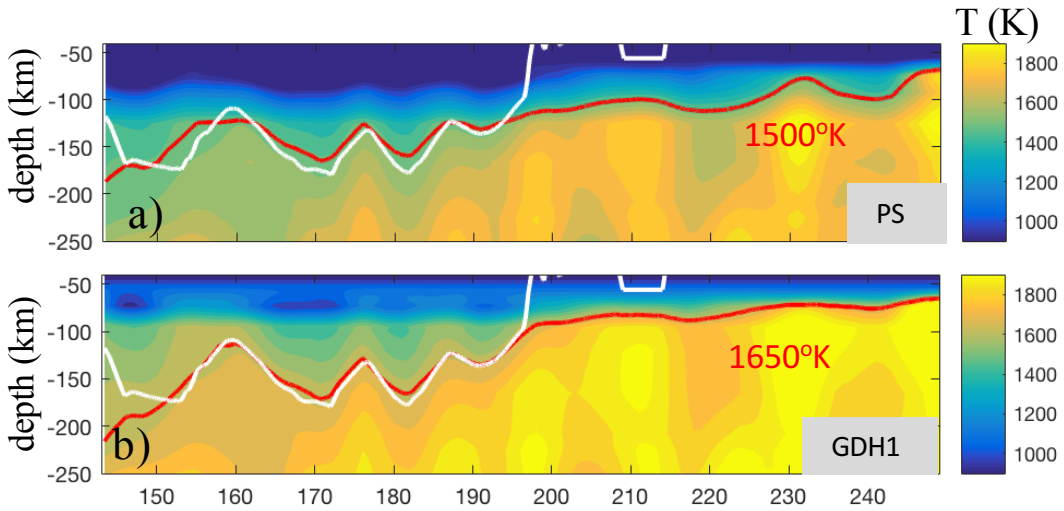

Figure S9: The color maps represent the temperature fields computed from models PS (a), and GDH1 (b). We assume a 0.5°/km thermal gradient beneath the lithosphere. The white line represents the base of the lithosphere determined by dvs=1.5%, and the red lines, isotherms computed from the two models (values reported in each panel).

3. Parameters of the geodynamic model

The physical values used in the geodynamic models are reported in table S1.

Table S1. Physical values used in this study

Meaning of symbols	Value
Model thickness, b	2900 km
Earth's radius, r_1	6371 km
Gravitational acceleration at the surface, g	9.81 m s^{-2}
Reference density, ρ_0	3350 kg m^{-3}
Reference viscosity in the upper mantle, η_0	10^{21} Pa s
Reference thermal diffusivity, κ_0	10^{-6} m^2 s^{-1}
Instantaneous Rayleigh number, Ra_i	9.45×10^7 or 8.0×10^9
Density contrast between the mantle and sea water, $\Delta\rho_s$	2320 kg m^{-3}
Density contrast at the core-mantle boundary, $\Delta\rho_c$	4337 kg m^{-3}
Gravitational constant, G	6.66726×10^{-11} N m^2 kg^{-2}

References:

Adam C., King, S. D., Vidal, V., Rabinowicz, M., Jalobeanu, A., and Yoshida, M. (2015). Variation of the subsidence parameters, effective thermal conductivity, and mantle dynamics, Earth Planet. Sci. Lett., 426, 130–142

Bird, P., 2003. An updated digital model of plate boundaries. Geochem. Geophys. Geosyst. 4 (3), 1027.

Bodine, J., Steckler, M., et Watts, A. (1981). Observations of flexure and rheology of the oceanic lithosphere. J. Geophys. Res., 86, 3695–3707

French, S. W. and Romanowicz, B. A. (2014). Whole-mantle radially anisotropic shear velocity structure from spectral-element waveform tomography. Geophys. J. Int. 199, 1303-1327

Goetze, C. (1979). Stress and temperature in the bending lithosphere as constrained by experimental rock mechanics. Geophys. J. R. Astr. Soc., 59, 463–478.

Gripp, A.E., Gordon, R.G. (2002). Young tracks of hotspots and current plate velocities. Geophys. J. Int. 150, 321–361.

Isacks, B., Olivier, J., et Sykes, L. (1968). Seismology and the new global tectonics. J. Geophys. Res., 73, 5855–5899.

Karato, S.I. (2008). Deformation of Earth Materials: an Introduction to the Rheology of Solid Earth. Cambridge University Press, New York.

McNutt, M., et Menard, H. (1982). Constraints on the yield strenght in oceanic lithosphere derived from observations of flexure. Geophys. J. R. Astr. Soc., 71, 363–394.

McNutt, M. (1984). Lithospheric flexure and thermal anomalies. J. Geophys. Res., 89, 11,180–11,194.

Nishimura, C., et Forsyth, D. (1985). Anomalous Love-wave phase velocity in the Pacific : sequential pure path and spherical harmonic inversion. Geophys. J. R. Astr. Soc., 64, 389–407.

Parsons, B., and J. Sclater (1977). An analysis of the variation of ocean floor bathymetry and heat flow with age, J. Geophys. Res., 82, 803–827

Schubert, G., Turcotte, D.L., and Olson, P. (2001), Mantle Convection in the Earth and Planets, Cambridge: Cambridge University Press, 10.1017/CB09780511612879

Stein, C. S., and Stein, S. (1992). A model for the global variation in oceanic depth and heat flow with lithospheric age. Nature, 359, 123–129 https://doi.org/10.1038/359123a0

Turcotte, D., and Schubert, G. (1982). Geodynamics - Applications of continuum physics to geological problems. John Wiley and Sons. (450 p.)